ARTICLES
PUBLISHED ONLINE: 22 MAY 2017 | DOI: 10.1038/NNANO.2017.74
nature nanotechnology

Nanofluidic device for continuous multiparameter quality assurance of biologics

Sung Hee Ko[1], Divya Chandra[2], Wei Ouyang[1], Taehong Kwon[1], Pankaj Karande[2] and Jongyoon Han[1,3,4]*

Process analytical technology (PAT) is critical for the manufacture of high-quality biologics as it enables continuous, real-time and on-line/at-line monitoring during biomanufacturing processes. The conventional analytical tools currently used have many restrictions to realizing the PAT of current and future biomanufacturing. Here we describe a nanofluidic device for the continuous monitoring of biologics' purity and bioactivity with high sensitivity, resolution and speed. Periodic and angled nanofilter arrays served as the molecular sieve structures to conduct a continuous size-based analysis of biologics. A multiparameter quality monitoring of three separate commercial biologic samples within 50 minutes has been demonstrated, with 20 μl of sample consumption, inclusive of dead volume in the reservoirs. Additionally, a proof-of-concept prototype system, which integrates an on-line sample-preparation system and the nanofluidic device, was demonstrated for at-line monitoring. Thus, the system is ideal for on-site monitoring, and the real-time quality assurance of biologics throughout the biomanufacturing processes.

In the modern pharmaceutical industry, the term 'biologics' is used for engineered macromolecular products (or therapeutic proteins), such as monoclonal antibodies, cytokines and growth factors[1,2]. Biologics can provide an effective means for the treatment of serious diseases, such as rheumatoid arthritis, cancer, diabetes and various chronic diseases[3–7]. It is reported that the biologics market will reach $178.4 billion in 2017, and biologics account for seven of the top ten best-selling drugs listed in 2014 (refs 8,9). Owing to a much larger size and more-complex structure of biologics compared with small-molecule drugs[2], their properties are highly sensitive to manufacturing, handling and storage conditions[10]. Even a subtle chemical modification (for example, changes in glycosylation, oxidation, deamidation, isomerization, peptide bond cleavage, hydrolysis and so on) may compromise the efficacy and safety of biologics, or even provide the potential for life-threatening side effects[11,12]. Therefore, proper and robust quality assessments are essential throughout the entire manufacturing and delivery chain.

Currently, the critical quality attributes (CQAs) of biologics are measured only at the end of the lengthy biomanufacturing process, which forces significant delays in the product release (even when CQAs are assured) and the possibility of a significant disruption in the production if any CQA issues are discovered. For an effective productivity and quality control (that is, early fault detection), it is essential to monitor raw and in-process materials at all stages of the manufacturing process (also known as real-time CQA monitoring)[13,14].

The existing analytical tools for CQA monitoring, which include spectroscopic technologies, capillary electrophoresis and HPLC, are not ideally suited for real-time monitoring[15]. Spectroscopic technologies require significant data processing (correlation based) to interpret the relationship between measured spectral information and target bioprocess variables[13]. Capillary electrophoresis and HPLC are inherently batch-analysis systems, so their adaptation into automated continuous analytics is not trivial[16,17]. As an alternative, micro- or nanofluidic biomolecule analysis chips that miniaturize these product-quality assurance steps have been proposed, as they can reduce the risk of degradation induced by unsuitable delivery and storage conditions[18–22] via on-site drug monitoring. Yet, these systems do not provide real-time and on-line/at-line monitoring functions specifically for multivariate analysis (both purity and activity) in a single operation.

Here we report a nanofluidic device that enables a comprehensive biologics quality assessment in which a continuous-flow and multivariate (size, folding and activity) analysis of the biomolecules is achieved. The device proposed here has a simpler operation and better performance (detection sensitivity and resolution), because we have integrated both protein concentration and size separation using nanofilters in a single device[23–25]. As the nanofilter structures are not subject to mechanical and/or chemical degradation, and the unique design allows a continuous-flow operation, the device can be operated stably for a long period of time and realize a real-time and at-line monitoring in the biomanufacturing systems. Furthermore, the nanofluidic device is also ideal for an on-site (point-of-care) biologics monitoring system because of the short operational time (less that one hour), and minimal sample volume. Therefore, the device in this paper can provide a significantly enhanced sensitivity, speed and automation for a quality assessment well beyond that possible with conventional techniques from manufacturing to patient administration.

Design and operation of the slanted nanofilter array

The nanofluidic devices used for drug analysis consist of periodically patterned shallow regions and deep regions, which are tilted from the direction of the main channel and applied electric field (Fig. 1a). On the application of an electric field along the x axis, negatively charged molecules are driven into the nanofilter array by either electrophoresis or electro-osmotic flow depending on the

[1]Department of Electrical Engineering and Computer Science, Massachusetts Institute of Technology, Cambridge, Massachusetts 02139, USA. [2]Department of Chemical and Biological Engineering, Rensselaer Polytechnic Institute, Troy, New York 12180, USA. [3]Department of Biological Engineering, Massachusetts Institute of Technology, Cambridge, Massachusetts 02139, USA. [4]BioSystems and Micromechanics (BioSyM) IRG, Singapore-MIT Alliance for Research and Technology (SMART) Centre 138602, Singapore. *e-mail: jyhan@mit.edu

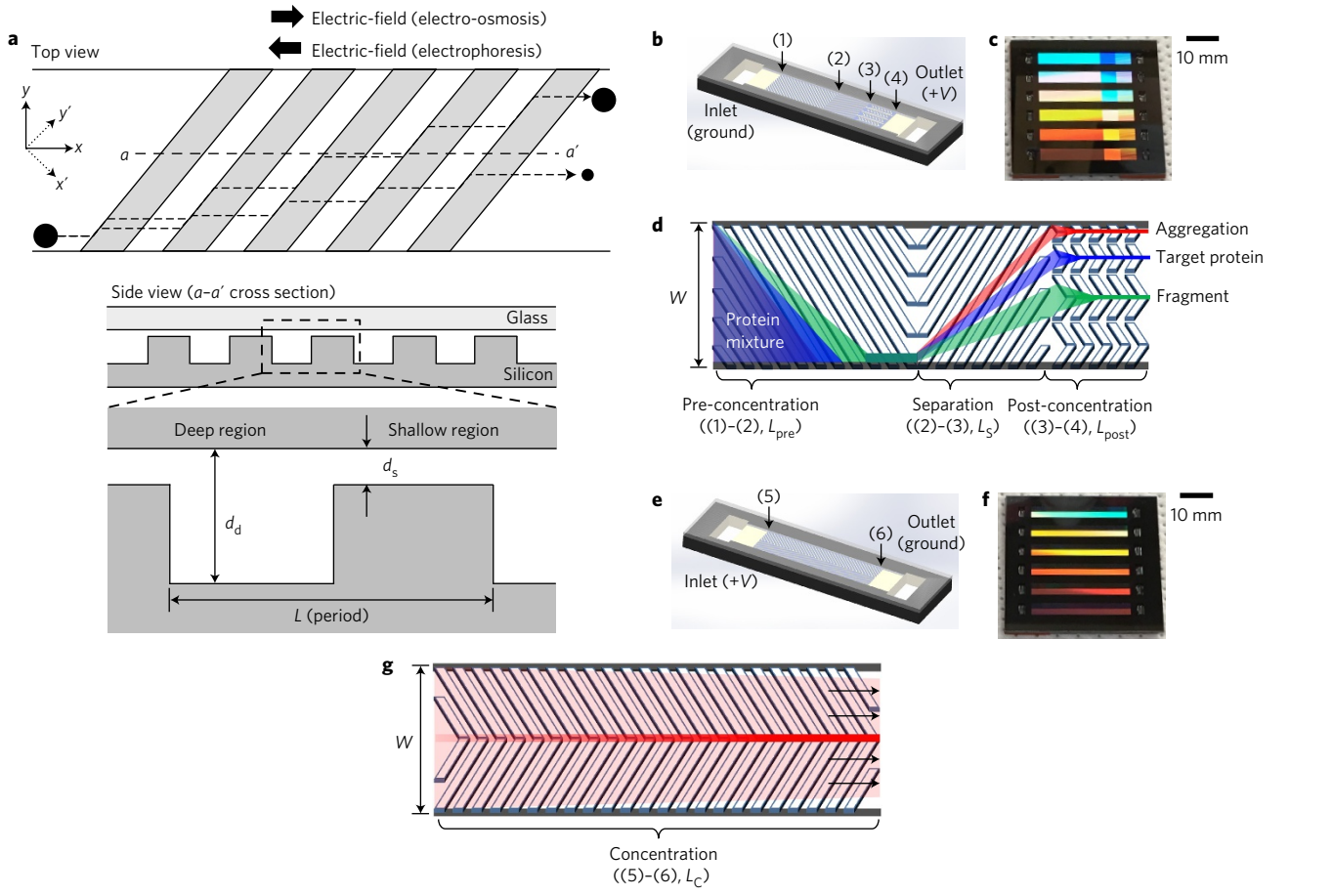

Figure 1 | Schematics of the slanted nanofilter array fabricated for both purity and bioactivity monitoring. a, Top and side views of the slanted nanofilter array. The device consists of periodic shallow (d_s) and deep (d_d) regions, and the period of the nanofilter (L) is 2 μm (shallow region, 1 μm; deep region, 1 μm). The top-view schematic shows size-dependent biomolecule behaviour in the nanofilter array (large filled circle, large biomolecule; small filled circle, small biomolecule). Arrows represent the direction of applied electric fields. **b**, Drawing of the drug purity monitoring device, which has one inlet and one outlet (+*V*, positive voltage). **c**, A silicon–glass chip that contains six channels with a width of 4 mm and individual inlets and outlets. **d**, A schematic of the nanofilter array structure and size-based separation of the proteins. The depth dimensions of the shallow and deep regions are 15 and 100 nm, respectively. Each channel consists of three regions, pre-concentration (length (L_{pre}) 2 cm and angle 135°), separation (length (L_S) 0.5 cm and angle 45°) and post-concentration (herringbone structure, length (L_{post}) 0.5 cm). *W*, width of the device. The SDS-denatured proteins travel through the nanofilter array by electrophoresis. **e**, Drawing of the bioactivity monitoring device. **f**, A silicon–glass chip for bioactivity monitoring. **g**, Schematic of the herringbone structure and the size-selective concentration of bound and unbound molecules. The depth dimensions of the shallow and deep regions are 30 and 100 nm in the peptide assay and 85 and 250 nm in the receptor assay, respectively. L_C, length of the concentration region. The red line shows the bound probe-molecule stream (concentrated), and the black arrows show the unbound probe-molecule stream (non-concentrated). The sample mixtures are driven by electro-osmotic flow.

buffer ionic strength and molecule surface charge[26,27]. Smaller molecules pass through the shallow region more easily than larger ones with a molecular size comparable to the nanofilter constriction, via the Ogston sieving effect[19,23,28]. In this system, molecule velocity (or mobility) by the electric field (along the *x* axis) can be decomposed into two orthogonal directions (x' and y' perpendicular and horizontal to the nanofilter direction, respectively), just as in the two-dimensional nanofilter array system[23]. The entropic force induced by the barrier between the deep and the shallow region affects only the velocity in the x' direction, which is perpendicular to the barrier of nanochannels[28], so that only the migration velocity in the x' direction decreases, depending on molecular size, and there is no velocity change in the y' direction. As a result, larger molecules have longer trapping times in the deep region, which leads to a longer migration in the y' direction before jumping across the shallow region (Fig. 1a). Therefore, different-sized molecules have their own deflection angle in the slanted nanofilter array, which leads to a continuous molecule sizing.

For drug-purity monitoring, the migration of molecules follows the direction of electrophoresis (Fig. 1b). The channel on the chip is divided into three regions, each of which is composed of nanofilter arrays with dissimilar angles and shapes (Fig. 1c,d). Molecules in the pre-concentration region are focused towards the bottom edge of the channel wall via the molecular sieving effect of the nanofilters. This region has two functions—one is to make molecules locate at the same position before being launched into the separation region[19,21], and the other is to concentrate molecules for an increased detection sensitivity. In the separation region, molecules are size separated as they move through the angled nanofilter array to form distinct molecular streams based on their size. To mitigate the molecular dispersion and the loss of detection sensitivity downstream, the post-concentration region is added to the downstream of the separation region, which re-concentrates each molecular stream separated and increases the detection sensitivity significantly. As the stream of each separated molecule has a different width, the post-concentration

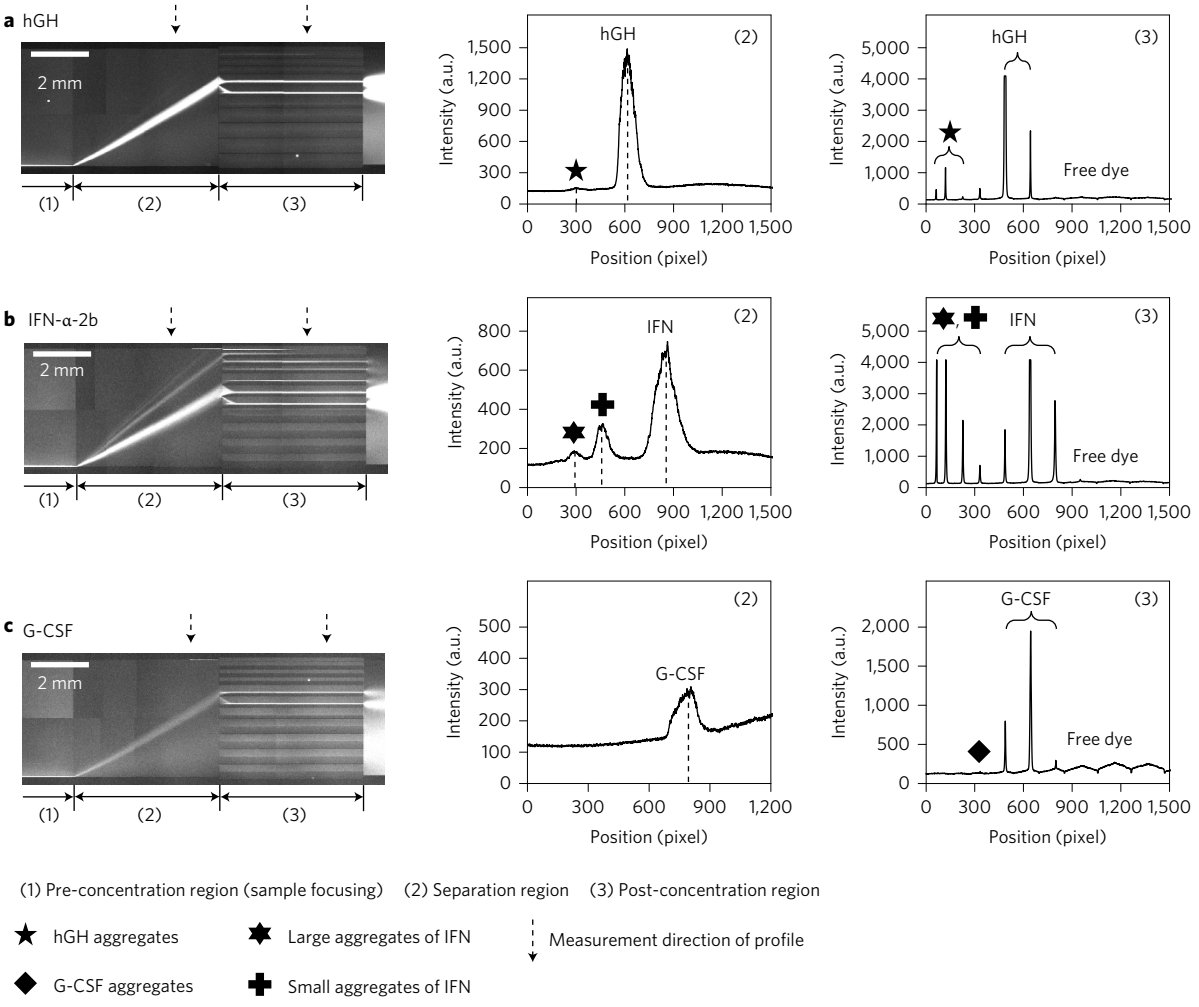

Figure 2 | Quantification of the limit of detection for three biologic drugs in the slanted nanofilter array system. a–c, hGH (22.1 kDa) (**a**), IFN (19.4 kDa) (**b**) and G-CSF (18.8 kDa) (**c**). After 50 min of applying the voltage (100 V), the stream line reaches a steady state. The exposure time is 500 ms. Each drug concentration is 100 μg ml^{-1}. The limit of detection of each biologic in the separation region was 0.2 μg ml^{-1} (hGH), 0.2 μg ml^{-1} (IFN) and 1 μg ml^{-1} (G-CSF). The limit of detection of each biologic in the post-concentration region was 0.05 μg ml^{-1} (hGH), 0.05 μg ml^{-1} (IFN) and 0.2 μg ml^{-1} (G-CSF) (Supplementary Section 1). The middle and right-hand columns show the profiles for the fluorescence stream line and the fluorescence intensity in the separation and post-concentration regions for hGH (**a**), IFN (**b**) and G-CSF (**c**).

region consists of channels with various widths to maximize the post-concentration effect. Each channel can collect only one species of separated molecules in a single channel. Additionally, it can minimize 'crossover' between different molecular species during the post-concentration stage.

The device design for bioactivity monitoring is similar to that for purity monitoring (Fig. 1e,f). After the mixture of target and probe molecules (binding partner) is loaded without the additional off-chip incubation step, electro-osmotic flow is applied to drive molecules into a herringbone nanofilter array in the channel (Fig. 1g). As the molecules are driven into the device, all of them are deflected and focused into a stream at the centre of the channel by the Ogston sieving effect[25]. In the case of extremely small probe molecules (for example, small peptide binders), only the bound probe molecules (large complexes) are selectively concentrated at the centre of the channel, whereas unbound probe molecules pass through the nanofilter array without deflection. When a probe molecule is larger than a certain size (for example, receptor or antibody), even the unbound probes can be concentrated, but the concentration factor of bound molecules is higher than that of the unbound molecules because of the size-selective sieving effect. By measuring the degree of concentration, one can realize a continuous, homogeneous binding assay between two proteins.

Continuous size-based separation and binding assay

To determine the achievable detection sensitivity and separation resolution of the device, a size-based separation was performed using three biological drugs along with protein molecular-weight markers. To evaluate the detection sensitivity, only a biologic drug solution was loaded into the device without protein markers. From the measured fluorescence profile, it was observed that the peak height of the post-concentration region is higher than that of the separation region (Fig. 2 and Supplementary Section 1). The limit of detection for each drug molecule was estimated by calculating the peak area at various concentrations (Supplementary Section 2), and was in the order of 50–100 ng ml^{-1} in the post-concentration region (varied depending on the labelling efficiency and other factors). The graphs show a linear relationship between the peak area and drug concentration, which allows a quantitative estimation of the concentration of the biologic drugs. In all three biologic drugs tested, minor aggregation peaks (marked with symbols) were detected because the drugs used here as samples have passed the expiration date or

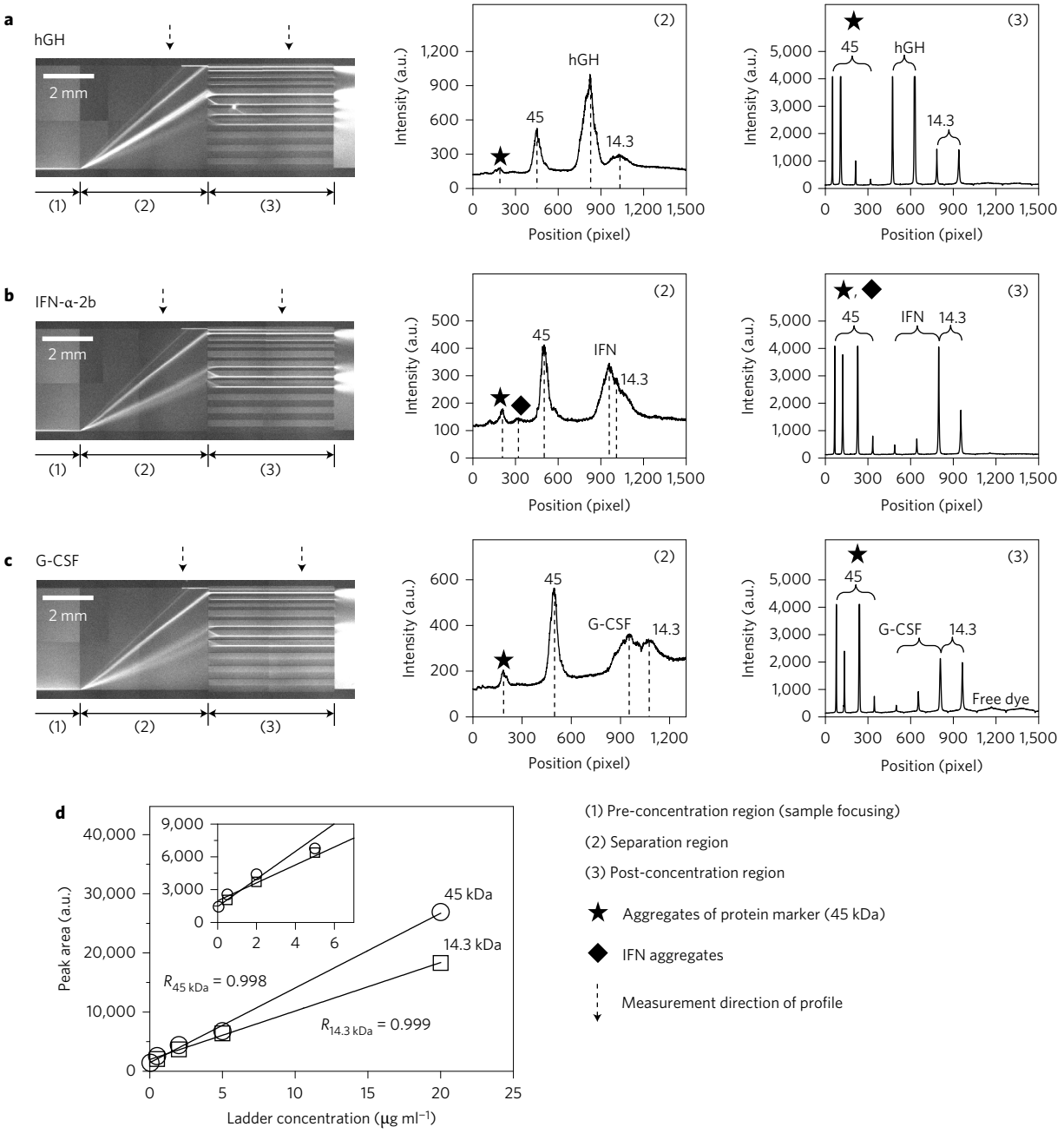

Figure 3 | Size-based separation of biologic drugs and protein markers in the slanted nanofilter array system. a–c, hGH (22.1 kDa) (**a**), IFN (19.4 kDa) (**b**) and G-CSF (18.8 kDa) (**c**). After 50 min of applying the voltage (100 V), the stream line reaches a steady state. The drug concentrations are 50 μg ml^{-1} (hGH), 20 μg ml^{-1} (IFN) and 100 μg ml^{-1} (G-CSF). The exposure time is 500 ms. The concentration of each protein marker is 20 μg ml^{-1}. Lower concentrations of drug were used in this experiment to prevent interference from pre-existing aggregation impurities. The middle and right-hand columns show the profiles for the fluorescence stream line and the fluorescence intensity in the separation and post-concentration regions for hGH (**a**), IFN (**b**) and G-CSF (**c**). **d**, Plot of peak area versus protein marker concentration in the separation region.

irreversible degradation may have occurred naturally after the manufacturing process[29]. The estimated detection sensitivity of nanofluidic size analysis matches or exceeds that of conventional protein-separation processes (Supplementary Section 3), with further enhancement (for example, simply by increasing the width of the channel, and therefore concentrating more molecules) and optimization possible. With this device, one can quantitatively monitor the aggregation of protein biologics down to 0.01 to 0.1% (the value depends on amount of single use for each drug), far below the level typically allowed (about 1–5% of total proteins[30–33]).

Separation resolution is another key factor to achieving a successful purity monitoring of biologic drugs, especially to detect potentially immunogenic protein aggregates[34,35]. Two protein markers with different molecular weights were selected to simulate impurities, such as aggregates and fragments. As the difference in entropic hindrance depends on the molecule size, each molecule has a certain deflection angle in the separation region. The separation performance between protein markers and the drug molecules indicates that the separation resolution is sufficient to monitor the aggregates and fragments (Fig. 3). The protein quantification also shows a linear relationship

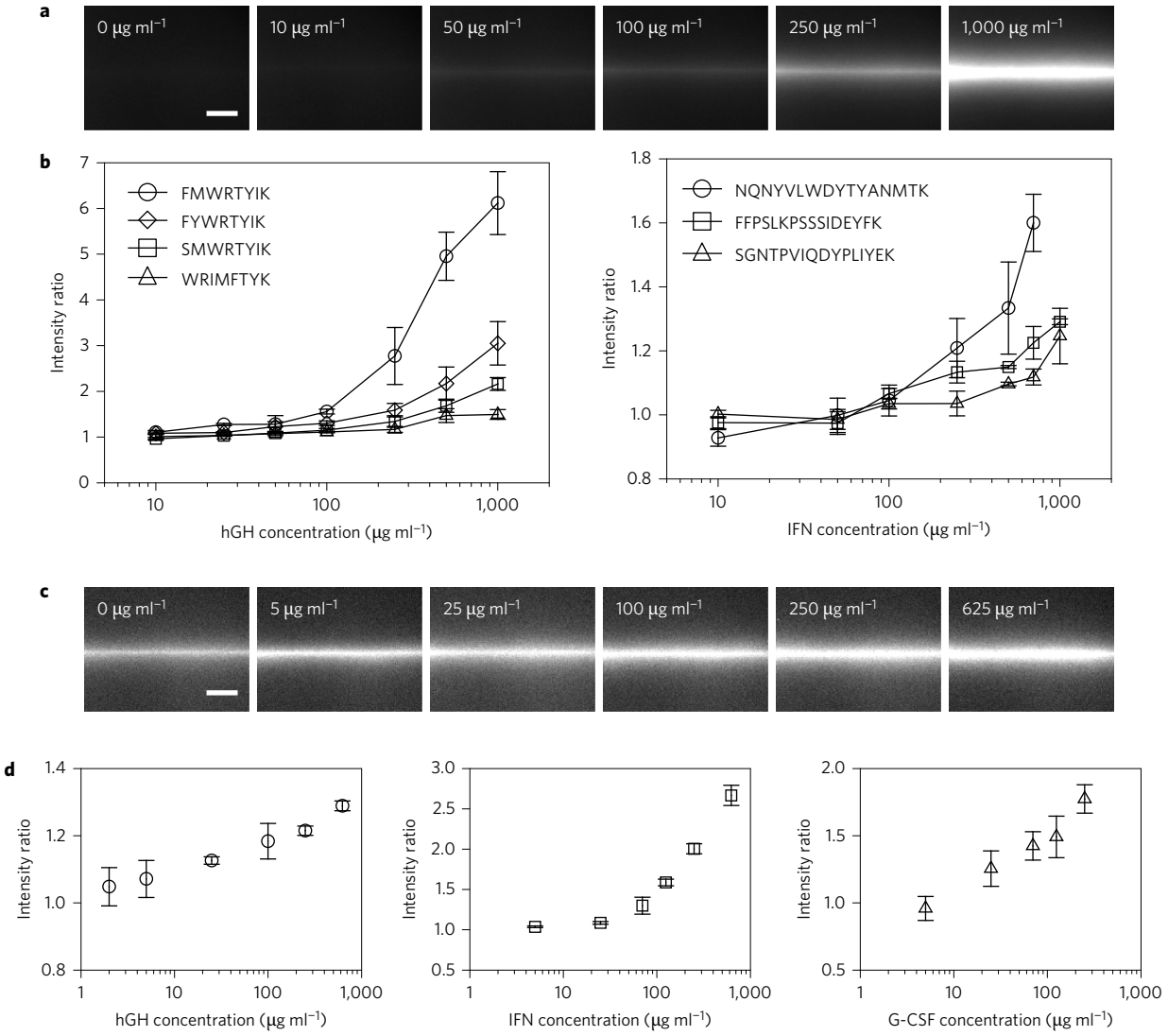

Figure 4 | Demonstration of homogeneous affinity binding assay using peptides and receptors for different drugs. a, hGH-peptide fluorescence bands concentrated in the centre of the channel with different hGH concentrations. Scale bar, 100 μm. **b**, Dose–response curve depending on concentrations of the drugs. Peptide concentrations for hGH and IFN were 20 and 30 μg ml^{-1}, respectively. Error bars represent the s.d. of three measurements. Peptide sequence for hGH: FMWRTYIK (circles), FYWRTYIK (diamonds), SMWRTYIK (squares) and WRIMFTYK (triangles). Peptide sequence for IFN: NQNYVLWDYTYANMTK (circles), FFPSLKPSSSIDEYFK (squares) and SGNTPVIQDYPLIYEK (triangles). **c**, hGH-receptor fluorescence bands concentrated in the centre of the channel with different hGH concentrations. Scale bar, 100 μm. **d**, Dose–response curve depending on the concentration of the drugs. The receptor concentrations for hGH (circles), IFN (squares) and G-CSF (triangles) were 25, 50 and 50 μg ml^{-1}, respectively. Error bars represent the s.d. of five measurements.

between the peak area versus molecular concentration (Fig. 3d and Supplementary Section 4).

To demonstrate the bioactivity assessment, both peptides and specific target receptors were used as probe molecules to provide multivariate (yet overlapping) information (folding versus activity) as to the biologic molecules. Free peptides (about 1–2 kDa) are relatively small compared with the depth of the nanofilter, so no appreciable concentration can occur in the nanofilter array, unless they are bound to much larger protein biologics. As we increase the drug concentration, focused fluorescence bands start to appear at the centre of the channel (Fig. 4a). Using the binding results, the dose–response curves were plotted for different drug molecules and peptides binders (Fig. 4b). These curves show that the binding increases with the addition of the drug, and each peptide has a differential binding affinity. Of them, FMWRTYIK (human growth hormone (hGH)) and NQNYVLWDYTYANMTK (interferon-γ (IFN)) showed the highest binding affinities. In addition to the peptides (binding to which may assure the proper folding of biologics), specific receptors were used as the probe molecule, because binding activity towards a cell-surface receptor would correlate with drug efficacy. For the size-selective differential concentration of free receptors versus drug–receptor complexes, a herringbone nanofilter array device with a larger gap size was used[25,27]. Larger drug–receptor complexes are concentrated more rapidly than free receptors, and therefore an increase in the band intensity at the centre of the channel can be used as the signal representative of the binding of the drugs to the receptors (Fig. 4c). The dose–response curves obtained (Fig. 4d) show that the assay is adequate for monitoring binding activity in the concentration range of about 10–1,000 μg ml^{-1}, which is relevant for most biologics manufactured for humans. The limit of detection for each drug was 2 μg ml^{-1} (hGH), 5 μg ml^{-1} (IFN-α-2b) and 5 μg ml^{-1}

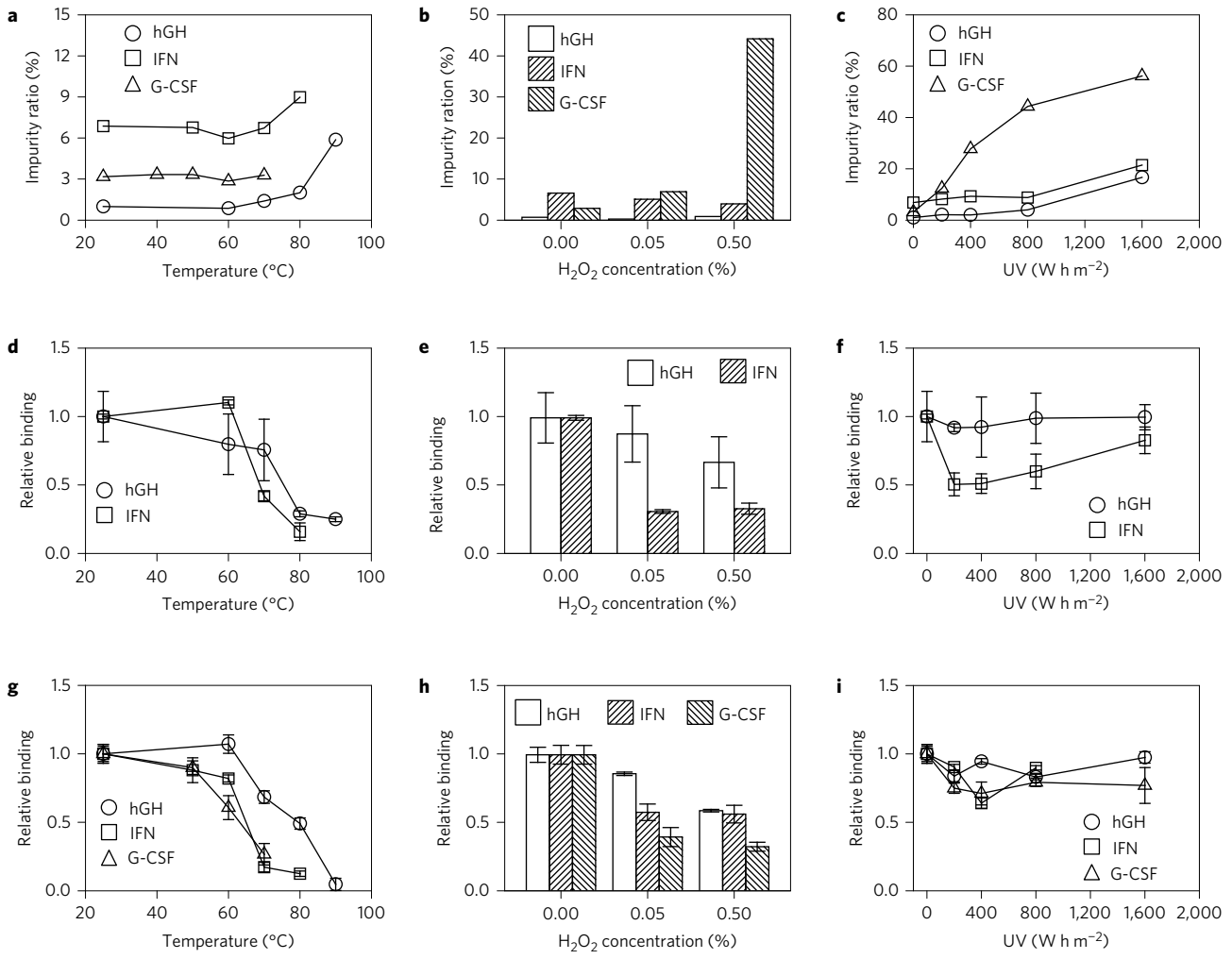

Figure 5 | Purity and bioactivity assessments of the forced degraded drugs hGH, IFN and G-CSF. a–c, Impurity ratio (aggregation ratio) for drugs treated by heat (thermal) (**a**), H_2O_2 (oxidation) (**b**) and ultraviolet light (UV) (**c**). Drug concentrations were 50 μg ml^{-1} (hGH), 20 μg ml^{-1} (IFN) and 100 μg ml^{-1} (G-CSF). For the affinity binding assay peptides FMWRTYIK (hGH) and NQNYVLWDYTYANMTK (IFN) were used, as they provide the highest binding affinity. Drug concentrations were 250 μg ml^{-1} (hGH) and 250 μg ml^{-1} (IFN). Peptide concentrations were 20 μg ml^{-1} (hGH) and 30 μg ml^{-1} (IFN). Error bar represents the s.d. of three measurements for the peptide binding assay. **d–f**, Relative binding activity value for drugs treated by heat (thermal) (**d**), H_2O_2 (oxidation) (**e**) and ultraviolet light (**f**). For the binding assay using receptors, cell-surface receptors were used. The drug concentrations were 250 μg ml^{-1} (hGH), 200 μg ml^{-1} (IFN) and 100 μg ml^{-1} (G-CSF). The receptor concentrations were 25 μg ml^{-1} (hGH), 50 μg ml^{-1} (IFN) and 50 μg ml^{-1} (G-CSF). **g–i**, Relative binding activity value using receptors for the drugs treated by heat (thermal) (**g**), H_2O_2 (oxidation) (**h**) and ultraviolet light (**i**). Error bar represents the s.d. of five measurements for the receptor-binding assay.

(granulocyte-colony stimulating factor (G-CSF)), which are adequate to evaluate the post-manufacturing biologics. In both bioactivity assessments, the binding reaction between the drug and probe molecules occurs in the solution phase and washing steps are not required, and therefore the assays are simpler and easier to run than surface-based binding assays.

Detection and quantification of biologic drug degradation

To demonstrate the functionality of the nanofilter array device in monitoring protein biologics degradation, after being degraded by the typical stress methods used in forced degradation, several biologics were tested using the device. Forced degradation is a standard method in industry to screen material stability rapidly as an alternative to stability tests over a long-term degradation in realistic storage conditions[36]. We applied our nanofluidic platform to monitor the quality of biologic drugs post-degradation. To achieve that, several forced degradation (stress-testing) methods were employed on the three biologic molecules, followed by an analysis in the nanofluidic device (size-based separation and binding assay via peptides and receptors).

When heating native biologics, an additional narrow streamline is observed above certain denaturation temperature (Supplementary Figs 4a,b, 5a,b and 6a,b). The intensity ratio of the streamlines (aggregation versus monomer) increases with temperature, and the critical temperatures around which aggregations start to show are 80 and 70 °C for hGH and IFN, respectively, whereas the ratio for the G-CSF is independent of temperature (Fig. 5a). Homogeneous binding assays show a general decrease in binding activity as the temperature increases (Fig. 5d,g and Supplementary Section 6). To simulate the oxidation-induced degradation, H_2O_2, a commonly used oxidant, was used, which resulted in the oxidation of methionine residues of the proteins[36]. Our results show that the aggregation impurity level in both hGH and IFN does not change significantly with the addition of H_2O_2, whereas the aggregation impurity level of G-CSF is highly correlated with the H_2O_2 concentration (Fig. 5b and Supplementary Figs 4c, 5c and 6c). However, the binding assay

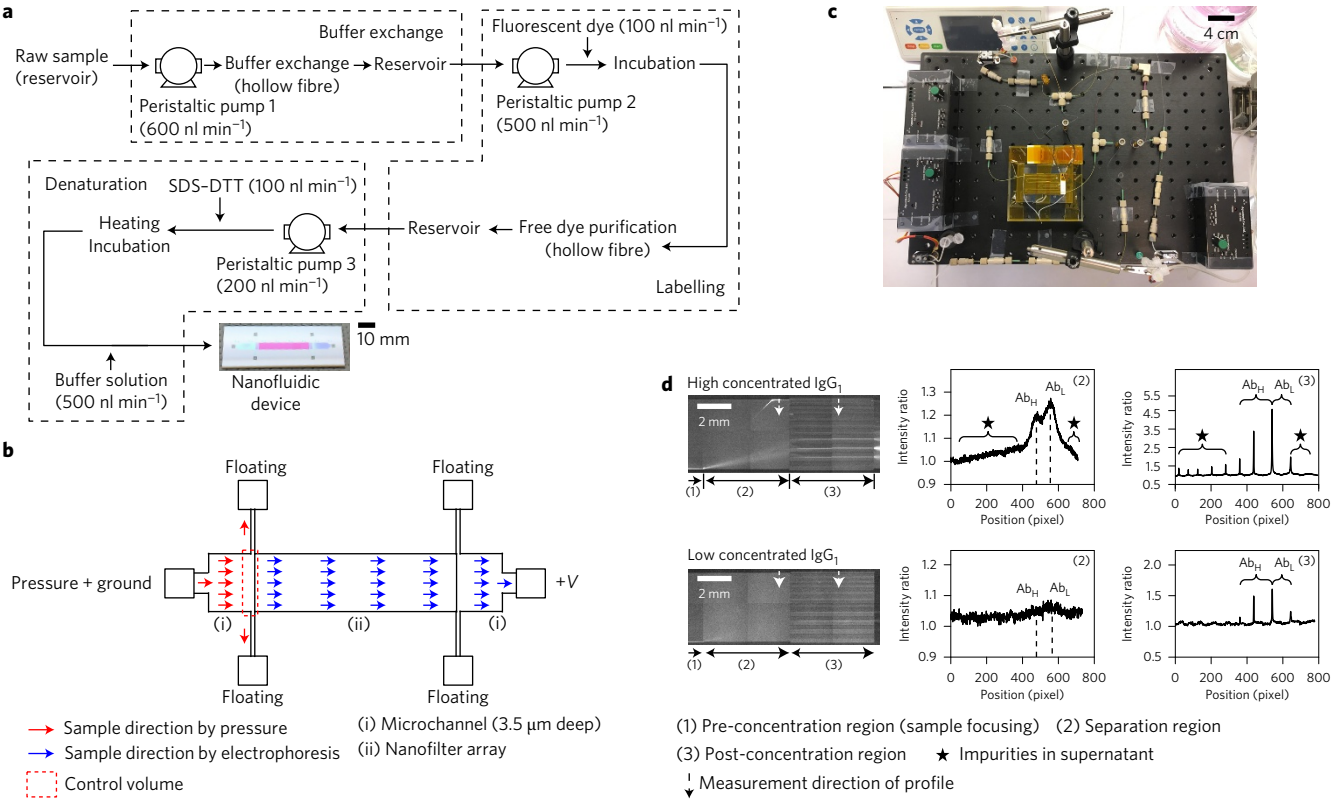

Figure 6 | Proof-of-concept prototype for the at-line purity assessment of supernatants of a CHO-K1 cell culture (~3.4 million cells per millilitre of batch culture) that contains antibody products (IgG1) using an on-line sample preparation system and the nanofluidic device (d_s of 20 nm and d_d of 100 nm). a, Overall workflow of on-line sample preparation and modified nanofluidic device. Each dashed line rectangle includes each process module (buffer exchange, labelling and denaturation). **b**, Direction of sample movement by each pressure-driven flow and electrophoresis inside the nanofluidic device ((i), microchannel region; (ii), nanofilter array). **c**, On-line sample preparation system. At the current prototype stage, this is a capillary-based continuous-flow reactor and mixer, which eventually leads to the nanofluidic device in which separation occurs. **d**, Fluorescence stream lines and fluorescence intensity profiles of supernatants in the separation and post-concentration regions. The IgG1 concentration in each supernatant is 375 μg ml^{-1} (high concentration of IgG1) and 120 μg ml^{-1} (low concentration of IgG1), respectively. The fluorescence signal was normalized by a background signal. The applied voltage is 200 V.

with the peptides and receptors present showed that the binding activity for all the target drugs decreased with the addition of H_2O_2 (Fig. 5e,h and Supplementary Section 7). The International Conference on Harmonisation guideline Q1B recommends that an ultraviolet range of 320–400 nm and a power of at least 200 W h m^{-2} be used as a source for forced photodegradation[37]. In purity analysis, all of the drugs are aggregated (non-covalent aggregation[36]) with increasing ultraviolet exposure power, especially severely in G-CSF (Fig. 5c and Supplementary Figs 4d, 5d and 6d). Binding activity assays show that the bioactivity for all the drugs is low compared with that of native drugs when they are photo-degraded, and the degree of bioactivity loss depends on the drug (Fig. 5f,i and Supplementary Section 8).

From the size-based separation and binding activity assay results, it was confirmed that the nanofilter array device is applicable to monitoring drug degradation, such as aggregation and loss of bio-activity, which are related to the purity (safety), potency and efficacy of the drug (Fig. 5). Some degradation results are identical with previously reported results, but others are different to them (Supplementary Sections 6–8). This is probably because of the different degradation conditions used in different works, as no standard procedure for forced degradation is available[36]. At the same time, for the protein solution with a significant aggregation present, the binding activity assay results can be skewed because of a rapid concentration of the aggregation with or without target binding (as seen in G-CSF irradiated by ultraviolet light). Still, it is clear that the combined set of rapid real-time assays presented here is capable of providing actionable information on the CQAs of the biologics solution at hand, with the sufficient sensitivity, specificity and speed necessary for next-generation biomanufacturing.

At-line monitoring system for purity assessment

One of the most important merits of our technology is the ability to monitor continuously a stream of supernatants that exit a bio-reactor. To demonstrate the at-line monitoring system for purity assessment, we designed an on-line sample-preparation system integrated with the nanofilter array device to analyse supernatants that contain immunoglobulin IgG1 (Fig. 6a–c and Supplementary Section 9). To load the treated sample directly into the nanofilter array device using a pressure-driven flow, additional microchannels were placed at both ends of the nanofilter array device (Fig. 6a,b) to address any flow mismatch. In the microchannel region, most of the incoming sample flew out through two side channels, because of the high hydrodynamic resistance of the nanofilter region. Nevertheless, sample solution was delivered near the entrance of nanofilter region, where protein molecules were introduced via electro-osmosis and/or electrophoresis. We obtained the first experimental data to analyse the bioreactor supernatants directly using the prototype system (Fig. 6d). It was confirmed that not only can the system monitor molecules in the supernatant, such as heavy chain (Abʜ), light chain (Abʟ) and impurities (aggregates and host-cell proteins because the samples were not purified through the downstream

process), but it can also monitor any change of biomolecule property, continuously and automatically (for example, different IgG1 concentrations, and different molecules, as shown in Supplementary Fig. 7c).

Conclusions

In response to the critical lack of real-time biologics product analysis, which would dramatically enhance the efficiency and safety of modern biologics manufacturing, we have developed a solid-state biologics CQA analysis system that can be interfaced directly with modern bioreactors. Several critical safety and efficacy metrics (aggregation, folding and binding activity) can be measured continuously, directly from the cell culture supernatant. Three independent tests were carried out for each sample and provided independent yet overlapping information regarding the biologics being tested. Nanofluidic size separation directly measures the presence of potentially immunogenic protein aggregates as well as of protein fragments (with a reduced efficacy). Peptide binding to the target, screened by the microarray screening method, can provide assurances on the proper folding and surface structure of the proteins. Finally, binding activity towards the specific cell-surface receptor is the most specific *in vitro* measurement used to assess bioactivity *in vivo*. Not only do the assay performance metrics meet or exceed the level necessary for a safety and efficacy assurance, but also many of them exceed those of the current state-of-the-art technology. These unique characteristics mean that not only does the slanted nanofilter array device allow a continuous-flow and one-step operation for biomolecule analysis, but also it can realize a truly 'real-time and on-line/at-line' CQA monitoring in biomanufacturing through integration with a continuous-flow sample preparation system (Fig. 6). In addition, different kinds of analyses (sizing, peptide binding and receptor binding) in a single chip that consists of multiple channels can be performed by adopting different nanofilter patterns and dimensions, all manufactured simultaneously via standard microfabrication processes (Fig. 1c,f).

The current on-line sample preparation system has a sample-to-assay delay time of five hours. Such a delay would still be manageable and acceptable in terms of modern bioreactor engineering, where important changes can occur over tens of hours. Yet, a further reduction of this time delay is definitely possible by optimizing the sample preparation workflow, including the use of a non-covalent dye or label-free detection method (for example, ultraviolet fluorescence), and integrating the sample preparation workflow in a microfluidic device (with a much smaller dead volume) instead of a capillary system. In the case of an activity assessment, as only a mixing step is required, the processing time delay is minimal (~20 minutes). Based on these results, we aim to integrate the system with a bioreactor to sample and monitor continuously the produced proteins directly from a bioreactor (Supplementary Fig. 7d). Many CQAs of importance can be continuously checked directly, which can be used to optimize and manipulate the process conditions continuously with a closed-loop feedback control.

Recently, an advanced biomanufacturing system that aimed to produce one dose of a drug in 24 hours was reported[38], and Adamo *et al.* demonstrated a modular, on-demand synthesis platform of small-molecule drugs, ideally suited for many scenarios in which traditional biomanufacturing is not adequate, technologically or economically[39]. Conventional analytical methods cannot be used to CQA test because of the limited amount of biologics produced in the next-generation bioprocessing modules. In addition, there are currently no mechanisms for the quality assurance between product release and drug administration to the patient, which is a safety challenge with several recent incidences. We believe that the nanofluidic system demonstrated in this work can fill these gaps, as it enables a rapid, point-of-care quality validation with a minimal amount of samples (<<1 μl).

Methods

Methods and any associated references are available in the online version of the paper.

Received 16 September 2016; accepted 17 March 2017; published online 22 May 2017

References

1. Rader, R. A. (Re)defining biopharmaceutical. *Nat. Biotechnol.* **26,** 743–751 (2008).
2. Baumann, A. Early development of therapeutic biologics-pharmacokinetics. *Curr. Drug Metab.* **7,** 15–21 (2006).
3. Leader, B., Baca, Q. J. & Golan, D. E. Protein therapeutics—a summary and pharmacological classification. *Nat. Rev. Drug Discov.* **7,** 21–39 (2008).
4. Taylor, P. C. & Feldmann, M. Anti-TNF biologic agents: still the therapy of choice for rheumatoid arthritis. *Nat. Rev. Rheumatol.* **5,** 578–582 (2009).
5. Menard, S., Pupa, S. M., Campiglio, M. & Tagliabue, E. Biologic and therapeutic role of HER2 in cancer. *Oncogene* **22,** 6570–6578 (2003).
6. Goeddel, D. V. *et al.* Expression in *Escherichia coli* of chemically synthesized genes for human insulin. *Proc. Natl Acad. Sci. USA* **76,** 106–110 (1979).
7. Guildford-Blake, R. & Strickland, D. *Guide to Biotechnology 2008* (Biotechnology Industry Organization, 2008).
8. Visiongain, *World Biological Drugs Market 2013–2023* (Visiongain, 2013).
9. EvaluatePharma, *World Preview 2015, Outlook to 2020* (EvaluatePharma, 2015).
10. Wang, W. Instability, stabilization, and formulation of liquid protein pharmaceuticals. *Int. J. Pharm.* **185,** 129–188 (1999).
11. Frokjaer, S. & Otzen, D. E. Protein drug stability: a formulation challenge. *Nat. Rev. Drug Discov.* **4,** 298–306 (2005).
12. Giezen, T. J. *et al.* Safety-related regulatory actions for biologicals approved in the United States and the European Union. *J. Am. Med. Assoc.* **300,** 1887–1896 (2008).
13. Teixeira, A. P., Oliveira, R., Alves, P. M. & Carrondo, M. J. T. Advances in on-line monitoring and control of mammalian cell cultures: supporting the PAT initiative. *Biotechnol. Adv.* **27,** 726–732 (2009).
14. Rathore, A. S., Bhambure, R. & Ghare, V. Process analytical technology (PAT) for biopharmaceutical products. *Anal. Bioanal. Chem.* **398,** 137–154 (2010).
15. Pais, D. A. M., Carrondo, M. J. T., Alves, P. M. & Teixeira, A. P. Towards real-time monitoring of therapeutic protein quality in mammalian cell processes. *Curr. Opin. Biotechnol.* **30,** 161–167 (2014).
16. Alhusban, A. A., Gaudry, A. J., Breadmore, M. C., Gueven, N. & Guijt, R. M. On-line sequential injection-capillary electrophoresis for near-real-time monitoring of extracellular lactate in cell culture flasks. *J. Chromatogr. A* **1323,** 157–162 (2014).
17. St Amand, M. M., Ogunnaike, B. A. & Robinson, A. S. Development of at-line assay to monitor charge variants of MAbs during production. *Biotechnol. Prog.* **30,** 249–255 (2014).
18. Hatch, A. V., Herr, A. E., Throckmorton, D. J., Brennan, J. S. & Singh, A. K. Integrated preconcentration SDS–PAGE of proteins in microchips using photopatterned cross-linked polyacrylamide gels. *Anal. Chem.* **78,** 4976–4984 (2006).
19. Fu, J., Mao, P. & Han, J. A nanofilter array chip for fast gel-free biomolecule separation. *Appl. Phys. Lett.* **87,** 263902 (2005).
20. Han, J. & Craighead, H. G. Separation of long DNA molecules in a microfabricated entropic trap array. *Science* **288,** 1026–1029 (2000).
21. Bousse, L. *et al.* Protein sizing on a microchip. *Anal. Chem.* **73,** 1207–1212 (2001).
22. Huang, L. R. *et al.* A DNA prism for high-speed continuous fractionation of large DNA molecules. *Nat. Biotechnol.* **20,** 1048–1051 (2002).
23. Fu, J., Schoch, R. B., Stevens, A. L., Tannenbaum, S. R. & Han, J. A patterned anisotropic nanofluidic sieving structure for continuous-flow separation of DNA and proteins. *Nat. Nanotech.* **2,** 121–128 (2007).
24. Yamada, M., Mao, P., Fu, J. & Han, J. Rapid quantification of disease-marker proteins using continuous-flow immunoseparation in a nanosieve fluidic device. *Anal. Chem.* **81,** 7067–7074 (2009).
25. Cheow, L. F., Bow, H. & Han, J. Continuous-flow biomolecule concentration and detection in a slanted nanofilter array. *Lab Chip* **12,** 4441–4448 (2012).
26. Han, J. & Craighead, H. G. Characterization and optimization of an entropic trap for DNA separation. *Anal. Chem.* **74,** 394–401 (2002).
27. Bow, H., Fu, J. & Han, J. Decreasing effective nanofluidic filter size by modulating electrical double layers: separation enhancement in microfabricated nanofluidic filters. *Electrophoresis* **29,** 4646–4651 (2008).
28. Fu, J., Yoo, J. & Han, J. Molecular sieving in periodic free-energy landscapes created by patterned nanofilter arrays. *Phys. Rev. Lett.* **97,** 018103 (2006).

29. Riggin, R. M., Dorulla, G. K. & Miner, D. J. A reversed-phase high-performance liquid chromatographic method for characterization of biosynthetic human growth hormone. *Anal. Biochem.* **167,** 199–209 (1987).
30. Riggin, R. M., Shaar, C. J., Dorulla, G. K., Lefeber, S. D. & Miner, D. J. High-performance size-exclusion chromatographic determination of the potency of biosynthetic human growth hormone products. *J. Chromatogr. A* **435,** 307–318 (1988).
31. Bodo, G., Maurer-Fogy, I., Falkner, E. & Lindner, S. J. Process for preparing and purifying alpha-interferon. US patent 5196323 A (1993).
32. Grabstein, K. H. & Morrissey, P. J. Treatment of bacterial diseases with granulocyte-macrophage colony stimulating factor (GM-CSF). US patent 5162111 A (1992).
33. Geigert, J. *The Challenge of CMC Regulatory Compliance for Biopharmaceuticals and Other Biologics* (Springer, 2013).
34. Mahler, H.-C., Friess, W., Grauschopf, U. & Kiese, S. Protein aggregation: pathways, induction factors and analysis. *J. Pharm. Sci.* **98,** 2909–2934 (2009).
35. Wang, W. Protein aggregation and its inhibition in biopharmaceutics. *Int. J. Pharm.* **289,** 1–30 (2005).
36. Hawe, A. *et al.* Forced degradation of therapeutic proteins. *J. Pharm. Sci.* **101,** 895–913 (2012).
37. International Council of Harmonisation. Guideline for the photostability testing of new drug substances and products. *Fed. Regis.* **62,** 27115–27122 (1997).
38. Lu, A. E. *et al.* Control systems technology in the advanced manufacturing of biologic drug. In *2015 IEEE Conf. Control Applications* 1505–1515 (2015).
39. Adamo, A. *et al.* On-demand continuous-flow production of pharmaceuticals in a compact, reconfigurable system. *Science* **352,** 61–67 (2016).

Acknowledgements

We thank P. Mao for providing advice on the nanofilter fabrication, the MIT Microsystems Technology Laboratories for support in the fabrication, P. W. Barone for discussion and assistance with the sample handling and J.-F. P. Hamel for his support in the cell culture and analysis. This work was mainly supported by the Defense Advanced Research Projects Agency and SPAWAR Systems Center Pacific (N66001-13-C-4025) to S.H.K., D.C., W.O., T.K., P.K. and J.H. a Siebel fellowship to W.O. and a Samsung Scholarship to T.K.

Author contributions

S.H.K. and J.H. conceived the project and S.H.K. designed and fabricated the device. S.H.K. conceived and performed the experiments for purity and activity monitoring with both non-degraded and degraded drugs using the at-line monitoring system and analysed the data. D.C. screened and provided peptide sequences for hGH and IFN, W.O. provided information on how to prepare the degraded drugs, T.K. cultured CHO-K1 cells in batch mode and provided IgG1. S.H.K. and J.H. wrote the manuscript, and J.H. and P.K. supervised the project.

Additional information

Supplementary information is available in the online version of the paper. Reprints and permissions information is available online at www.nature.com/reprints. Publisher's note: Springer Nature remains neutral with regard to jurisdictional claims in published maps and institutional affiliations. Correspondence and requests for materials should be addressed to J.H.

Competing financial interests

J.H. and S.H.K. have filed a patent application for the nanofilter device. P.K. and D.C. plan on filing patent applications for the peptide ligands.

Methods

Device fabrication. Nanochannel arrays on Si wafers (100) with various widths and depths were fabricated by standard photolithography and Si ion-reactive etching techniques, as described by Fu *et al.*[40]. In the photolithography process, a 5× reduction step-and-repeat projection stepper (Nikon NSR2005i9, Nikon Precision) was used to pattern nanochannels, which was followed by Si etching. To create access holes (reservoirs) to load samples and apply electric potentials, a thin nitride layer was deposited, by low-stress low-pressure chemical vapour deposition, on both sides of the silicon substrate, to provide an etch mask for KOH etching. The hole patterns were defined by photolithography and etching techniques, and then KOH etching was performed to etch through the silicon wafer to make the holes (20 wt% KOH solution at 80 °C). After stripping the nitride layer using a 49% HF solution, a 500 nm thermal oxide layer was grown as an electrical insulation between the Si wafer and the conducting buffer solution. To bond the silicon wafer and a flat glass substrate (Pyrex), a fusion-bonding process was chosen instead of anodic bonding. Fusion bonding tends to enable the fabrication of nanochannels as thin as 15 nm with a lower aspect ratio (depth/width)[41]. Both the silicon and the glass substrates were cleaned in piranha solution for 10 min, rinsed in deionized water and chemically treated by 29% ammonium hydroxide at room temperature for 30 min to form hydroxyl groups on the surfaces, which led to strong bonding in a spontaneous bonding process. After the substrates were rinsed and spin dried, two were contacted together by hand and pressed by a metal block (about 2.27 kg (5 lb)) overnight to enhance the bonding strength. To achieve an irreversible bonding of the pre-bonded substrates, an annealing process was conducted in a programmable furnace (Model BF51894C-1, Lindber/Blue M) at 550 °C for 12 h (temperature heating rate of 2 °C min^{-1}; cooling rate, 4 °C min^{-1}). Finally, the bonded substrates were cut by a die saw into individual devices. Before the bonding process, the depths and widths of the nanochannels were measured by atomic force microscopy. Additionally, a cross-section view of the nanochannels was further checked by scanning electron microscopy to investigate the change of nanochannel depth induced by the bonding process (Supplementary Section 10), but no significant changes were observed[41].

Samples and chemical reagents. Recombinant hGH, IFN-α-2b and G-CSF used for the drug analysis were supplied by Sandoz. The BSA (66 kDa), ovalbumin (45 kDa) and α-lactalbumin (14.3 kDa) were purchased from Sigma-Aldrich. To demonstrate at-line monitoring, IgG1 produced from CHO-K1 cells cultured in a batch mode bioreactor was used (Supplementary Section 11). The peptides used to demonstrate the binding assay were synthesized commercially (see below). The receptors for hGH and G-CSF (GHR-H5222 and GCR-H5223, respectively), were purchased from ACRO Biosystems. The IFN-α-2b receptor was purchased from Sino Biological Inc. (10359-H08H). Tris-borate-EDTA 10× (TBE), sodium bicarbonate, sodium dodecyl sulfate (SDS) and sodium bicarbonate were purchased from Sigma-Aldrich. The POP-6 polymer-CG (POP-6), dithiothreitol (DTT), PBS (pH 7.2), Alexa Fluor 488 dye and Alexa Fluor 555 dye were purchased from Invitrogen. The purification resin used to remove free dye was purchased from Bio-Rad (P2-gel).

Peptide design and synthesis for microarray screening. A library of peptides based on the two naturally occurring binding partners of hGH was designed for the initial screening and identification of hGH-binding peptides. The two hGH-binding receptor proteins employed in this study were the hGH receptor and the prolactin receptor. Peptides that spanned a length of 7–21 amino acids (aa) were designed based on the primary amino acid sequences of these two proteins. The library consisted of a total of 384 peptides. Similarly, for IFN-α-2b, peptides were designed by carrying out epitope mapping on IFN-α receptor 1 (IFNAR1) and receptor 2 (IFNAR2). Peptides with a length of 15 aa and a shift of 2 aa were designed such that two consecutive peptides in the library had an overlap of 13 aa. A total of 522 peptides was synthesized as part of the IFN-α-2b peptide library. For the microarray screening experiments to identify promising lead candidates that bound hGH or IFN-α-2b, peptides were synthesized on Celluspot discs (Intavis) using an automated, high-throughput peptide synthesizer (Multipep RS). Detailed information related to the synthesis of peptides on Celluspot has been reported previously[42]. Briefly, peptides were synthesized from their C- to N-termini using standard Fmoc chemistry. Post-synthesis, the peptide side-chain protecting groups were removed and peptide–cellulose conjugates were dissolved in dimethylsulfoxide and printed on microscope slides using a microarray printer. Further description of the microarray screening and subsequent in-solution validation (via fluorescence polarization) of the lead peptides selected to monitor bioactivity in the microfluidic assay is provided in Supplementary Sections 12 and 13.

Forced drug (protein) degradation. Before the drug degradation, all the drugs were diluted to a certain concentration from stock solutions by adding the TBE buffer solution. In the purity assessment, hGH, IFN-α-2b and G-CSF were diluted to 500, 400 and 800 μg ml^{-1}, respectively, whereas the concentrations of the three drugs were 1 mg^{-1} in the activity assessment (both peptide- and receptor-binding assay). For thermal treatments, four samples of 50–70 μl for each drug were prepared, and then incubated in the heating block for 30 min at various temperatures (50–90 °C). All the heated drug samples were cooled down to room temperature. Protein degradation carried out by the heating block and water bath resulted in no detectable differences. For light exposure, an ultraviolet transilluminator (Spectrolin, model number: TC-365R) with a range of 320–400 nm and a power of 375 W m^{-2} was used to treat the drug samples. Four samples for each drug were exposed in the ultraviolet transilluminator for 32, 64, 128 and 256 min, and the total energy absorbed was 200, 400, 800 and 1,600 W h m^{-2}, respectively. For oxidation, hydrogen peroxide at different concentrations of 0.05 and 0.5% was added to samples of each drug, and the samples were incubated in a water bath for 2 h at 37 °C. After incubation, drug samples were cooled down to room temperature. To quantify the aggregation level induced by forced degradation, the peak areas of the aggregates and the monomer in the post-concentration region were compared. Also, the relative binding ratio in the affinity binding assay was calculated by subtracting the background signal from the binding signal, depending on the degradation condition.

Size-based drug separation (purity assessment). To visualize the protein samples fractionated by the nanofilter array, drugs and protein standards (ovalbumin and α-lactalbumin) were labelled by Alexa Fluor 488 dye. Before adding the labelling dye into the protein samples, a buffer exchange was performed by using spin desalting columns with 7K MWCO (Pall Corporation) to change the sample buffer to 0.1 M sodium bicarbonate (pH 8.4), which leads to the highest labelling efficiency (Invitrogen). Then, Alexa Fluor 488 was added into the sample solutions, and the reaction mixtures were incubated for 1 h at room temperature with continuous stirring. After incubation, the mixtures were transferred to microfilter centrifugal devices (Pall Corporation) that contained purification resins (Bio-Gel P-2 Gel, Bio-Rad) to remove unreacted free dye. Finally, sample concentration and labelling efficiency were measured and calculated by a NanoDrop (ND-1000, Thermo Scientific).

Denaturation of drugs and protein standards was performed by adding 4 wt% SDS and 1 M DTT into the labelled samples. After mixing thoroughly, the SDS–DTT mixtures were incubated in an 80 °C heating block for 10 min, and then the mixtures were cooled down to room temperature. The SDS–proteins were diluted by adding 10× TBE buffer to obtain the desired SDS–protein concentration. The final concentrations of SDS and DTT were 0.05 wt% and 50 mM, respectively.

Silicon rubbers were placed on the silicon surface where there were buffer access holes to form reservoirs (Supplementary Section 14). The device was filled with 10× TBE, and an electro-osmotic flow was applied to remove trapped air bubbles inside the device[40]. To prevent nonspecific binding, a surface passivation solution of 10× TBE and 0.1 wt% POP-6 was injected into the device by electro-osmotic flow for 2 h (ref. 43). Then, it was washed by only the 10× TBE for 1 h. Finally, the device was filled with a mixture of 10× TBE and 0.05 wt% SDS immediately before the experiments were performed.

After loading the sample into the inlet reservoir and fresh buffer (mixture of TBE and SDS) into the outlet reservoir, both reservoirs were wrapped completely with parafilm to prevent evaporation during the experiments. The electric field was applied through platinum electrodes (Sigma-Aldrich) immersed in both reservoirs, which were connected to a source meter (Keithley 2400) to monitor the current flowing through the nanofilter arrays. An inverted epifluorescence microscope equipped with a cooled CCD (charge-coupled device) camera (Sensicam QE, PCO) was used for fluorescence images, and a 100 W mercury lamp was used as an illuminator. The samples labelled by Alexa Fluor 488 dye were visualized with a fluorescein isothiocyanate filter set ($\lambda_{ex}/\lambda_{em}$, 482 nm/536 nm, Semrock). Analysis of the images was performed by using ImageJ (NIH) and Matlab software.

Size-based drug concentration (activity assessment). To use a receptor in the binding assay, all the receptors were labelled by Alex Fluor 488 in the same way as the drug and protein standards were labelled. The only difference was that the lyophilized receptors had to be dissolved in a 0.1 M sodium bicarbonate solution in lieu of buffer exchange. The device-preparation process is the same as that described in the previous section. Instead of a mixture of TBE–SDS, only 7.5× TBE was used as buffer solution.

In the binding assays using either a peptide or a receptor, first, a non-labelled drug and peptide or receptor were mixed thoroughly by pipetting up and down in the microtubes (Supplementary Section 15). The mixtures were loaded into the inlet reservoir, without additional incubation in the microtube, and then an electric field was applied. After 1 h, fluorescence images were captured and analysed by the same equipment and software as described in the previous section.

On-line sample-preparation system. The on-line sample-preparation system for a continuous purity analysis consists of peristaltic pumps, a syringe pump, on-line microdialysis systems, a metal ceramic heater and a capillary tube. Microperistaltic pumps (RE-C100, Takasago Fluidic Systems) were used to deliver both raw and treated samples to the next sample-preparation step and a low-flow peristaltic pump (P720, Instech) was used for the buffer exchange and free dye removal in two on-line dialysis systems. To supply the chemical reagents (fluorescence dye, 1% SDS and 0.1 M DTT) and buffer solution (10× TBE), syringes of different size were used to induce different flow rates in one syringe pump (fusion 400, Chemyx). To achieve a continuous buffer exchange (to increase the labelling efficiency) and free dye removal in the labelling process, on-line microdialysis systems were fabricated using hollow fibre membranes (MWCO 3 kDa, diameter of 500 μm), which were taken from tangential flow filtration modules (mPES MicroKros Modules, Spectrum) and tube connectors (Harvard Apparatus)[44]. Sodium bicarbonate (100 mM) and 1× PBS (pH 7.2) were used for the buffer exchange and free dye removal, respectively. A metal ceramic heater (HT24S2, Thorlabs) controlled by a d.c. power supply and resistance temperature detector (TH100PT, Thorlabs) were used to heat a mixture of labelled sample and

chemical reagents (1% SDS and 0.1 M DTT) for sample denaturation. All the modules for the continuous-flow sample preparation were connected by capillary tubes with inner diameters of 100 and 150 μm, whereas tubes with an inner diameter of 1 mm were used for incubation of the fluorescence dye and the buffer exchanged sample.

Data availability. All the data generated or analysed during this study are included in this article and the Supplementary Information.

References

40. Fu, J., Mao, P. & Han, J. Continuous-flow bioseparation using microfabricated anisotropic nanofluidic sieving structures. *Nat. Protoc.* **4,** 1681–1698 (2009).
41. Mao, P. & Han, J. Fabrication and characterization of 20 nm planar nanofluidic channels by glass–glass and glass–silicon bonding. *Lab Chip* **5,** 837–844 (2005).
42. Chandra, D., Morrison, C. J., Woo, J., Cramer, S. & Karande, P. Design of peptide affinity ligands for S-protein: a comparison of combinatorial and *de novo* design strategies. *Mol. Divers.* **17,** 357–369 (2013).
43. Wang, Y. M. *et al.* Single-molecule studies of repressor–DNA interactions show long-range interactions. *Proc. Natl Acad. Sci. USA* **102,** 9796–9801 (2005).
44. Sun, L. *et al.* A facile microdialysis interface for on-line desalting and identification of proteins by nano-electrospray ionization mass spectrometry. *Rapid Commun. Mass Spectrom.* **22,** 2391–2397 (2008).